IEEE Access
Multidisciplinary | Rapid Review | Open Access Journal

Received June 3, 2020, accepted June 21, 2020, date of publication June 29, 2020, date of current version July 9, 2020.

Digital Object Identifier 10.1109/ACCESS.2020.3005657

Self-Tuning Multi-Transmitter Wireless Power Transfer to Freely Positioned Receivers

XIAOJIE DANG[1], PRASAD JAYATHURATHNAGE[2], (Member, IEEE), SERGEI A. TRETYAKOV[2], (Fellow, IEEE), AND CONSTANTIN R. SIMOVSKI[2]

[1]School of Electronic Engineering, Xidian University, Xi'an 710071, China
[2]Department of Electronics and Nanoengineering, School of Electrical Engineering, Aalto University, FI-00076 Aalto, Finland

Corresponding author: Xiaojie Dang (xjdang@mail.xidian.edu.cn)

ABSTRACT Free positioning of receivers is one of the key requirements for many wireless power transfer (WPT) applications, necessary from the end-user point of view. However, realization of stable and effective wireless power transfer for freely positioned receivers is technically challenging because of the need of complex control and tuning circuits. In this paper, we propose a concept of power channeling via an array of repeaters that enables self-tuning of multi-transmitter WPT systems without any sensing or control elements. The proposed WPT system consists of uncoupled transmitters and uncoupled repeaters which form independent power transfer channels. The proposed self-tuning WPT system is capable of maintaining stable output power with constant high efficiency regardless of the receiver position. Namely, our numerical and experimental results for a four-transmitter WPT system in form of a linear array show the efficiency $94.5 \pm 2\%$ for any position of the receiver within 20 mm range.

INDEX TERMS Wireless power transfer, overlapping coils, multiple transmitter coils, free positioning.

I. INTRODUCTION

Wireless power transfer (WPT) technology has attracted increased attention in many applications such as electric vehicles, medical implant devices, consumer electronics, and industrial applications, due to its numerous advantages. However, there are several technical challenges to overcome for wide and successful deployment of the WPT technology, which make the WPT technology an important research topic.

From the user view point, one of the key limitations in WPT applications is the requirement of perfect alignment between the transmitter (Tx) and the receiver (Rx). For example, in case of consumer electronics applications, such as wireless charging of mobile phones, laptops, tablet PCs, etc., free positioning of charged devices is most desirable, so that one can put the mobile device in an arbitrary position still ensuring efficient wireless charging without worrying about perfect alignment. In emerging new WPT applications such as WPT enabled kitchen appliances, WPT enabled furniture, or WPT for lighting applications, the user would prefer to have a large area enabled with wireless charging. Therefore, the requirement of free positioning in WPT applications is becoming more and more critical.

The associate editor coordinating the review of this manuscript and approving it for publication was Ting Yang.

A number of approaches have been proposed to enable free positioning of WPT receivers over a large area. All these proposals can be broadly categorized into two types: the use of large transmitting coil structures to generate a uniform magnetic field distribution over a large area, or the use of multiple transmitters to cover a large area. The first approach is simple and straightforward, however, it suffers from inferior efficiency due to very weak coupling between the Tx and Rx. For example, Liu *et al.* employ a combination of concentrated winding and spiral winding to design the transmitter and realize a uniform magnetic field [1]. However, the efficiency is about only 50% in the presence of one receiver. A smart multi-coil approach is proposed in [2] where a single Tx coil is coupled with multiple parrallelly connected resonators to enable large-area power transfer. However, such approaches still suffer from the decrease of efficiency with the increase of the power reception area.

Therefore, the use of multiple transmitter coils is the preferred method for most of the applications [3]–[7]. However, the excitation of Tx coils has become a complex problem. The simplest way is to excite all the Txs simultaneously [6]–[8]. However, such simultaneous and homogeneous activation is not optimal because different transmitting coils have different levels of coupling with the receiver. In fact, the optimal ratio of Tx coil currents depends on the mutual inductance of

every Tx-Rx pair [9], [10]. Therefore, simultaneous activation of many transmitters incur unnecessary power losses in those transmitters which are weakly coupled with the receiver. There have been several proposals to deactivate or suppress the currents in weakly coupled transmitters such as the use of additional on-off switches [11], [12], switchable compensation circuits [13], and additional switchable coupled-loops [14]. There have been several proposals to estimate mutual inductance using the voltage and current measurements from both Tx and Rx sides [15], [16]. Such methods require a continuous control and a wireless communication link between Tx and Rx. On the other hand, detection of Rx presence and mutual inductance estimation can be done by using only Tx side measurements in a single-Tx WPT system [17]–[19]. However, all these mutual inductance estimation techniques require additional control circuitry to regulate the power flow from several Txs and the Rx. Therefore, the requirement of the Rx position detection, complex control approaches, and additional tuning circuits have become the critical concern for selective activation of coils in multi-Tx WPT devices.

This paper proposes a self-tuning multi-Tx WPT system capable of automatic optimal power channeling through nearest Rx and Tx coils without any sensing or control circuits. The self-tuning property ensures that the power taken from each Tx coil is directed automatically to the proper Rx because this power is proportional to the square power of the coupling strength between that Tx and the Rx. The suggested approach got inspiration from the known idea of so called ''superlens'' based on two parallel arrays of small resonant objects [20], [21]. In that device, the resonators in each array are decoupled from each other, while there is near-field coupling between two parallel arrays. As shown in [20], [21], a small antenna positioned on one side of such parallel arrays excites resonant oscillations in the arrays so that there is a hot spot on the other side of the arrays located at the line drawn from the source orthogonally to the arrays. When the position of the source antenna changes, the hot spot on the other side of the arrays ''moves'', following the movement of the source. It means that this arrangement of resonators realizes point-to-point channels for energy for arbitrarily positioned sources. In earlier works, this feature was used for imaging applications [22], [23], but this functionality is critically important for WPT systems for freely positioned receivers, which we introduce here. The proposed WPT system consists of multiple Tx-repeater pairs, which are referred to as *independent channels* in this paper. The proposed WPT system realizes a uniform high-efficiency and stable output power throughout all Rx positions within the coverage area. The physical arrangement of the coils can be in any form as long as the following requirements are met: 1. All the coils except ones in the same channel are uncoupled from each other, and 2. For a given channel, coupling between the Tx and the Rx is small as compared to the coupling between the repeater and the Rx. Even though the ideal conditions may not be perfectly satisfied in practical implementations, we show that the concept of power channeling can be achieved with a proper design and optimization. A prototype implementation is numerically and experimentally verified in this paper. A transmitter array and a repeater array are formed by using a set of partially overlapping spiral coils with very weak cross coupling between them. The experimental results show that stable high efficiency can be maintained for arbitrary receiver positions without using any sensing, tuning, or control. Compared to the smart multi-coil approach with a single Tx coil suggested in [2], our method allows us to use an arbitrary number of transmitting coils either connected in parallel to a single power source or connected to separate power sources individually. This makes the proposed approach equally suitable for moderate power and high power applications. Meanwhile, the approach of [2] is hardly suitable for high-power transfer. Importantly, the proposed concept can be scaled to different types of multi-Tx WPT schemes that enable wireless charging of freely positioned receiver for diverse applications, such as 2D pad-like arrangement for consumer electronics applications, or 3D arrangement for wearable electronics applications.

The paper is organized as follows. In Section II, we analyze single Tx-Rx WPT systems including the conventional 2-coil WPT system and the 3-coil WPT system with a repeater, and find a simplified expressions for the currents in each coils, providing the basis for understanding the proposed automatic power channeling. In Section III, we discuss and analyze the concept of the proposed WPT scheme with respect to the coils currents, output power stability, and the efficiency characteristics. Section IV presents experimental results to verify the property of automatic self-switching between the corresponding power channels with small variations of the output power and efficiency. Finally, this paper concludes with a summary of the results in Section V.

II. WIRELESS POWER TRANSFER SYSTEM WITH A SINGLE TRANSMITTER AND RECEIVER

A. THE 2-COIL WPT SYSTEM

We start our discussion with the analysis of the 2-coil WPT system that includes a single Tx-Rx pair. The equivalent circuit of the WPT system is shown in Fig. 1(a), where two coils are connected to series compensation capacitors $C_{\rm tx}$ and $C_{\rm rx}$. Tx is excited by a voltage source $V_{\rm s}$ and the Rx is connected to an electrical load with an impedance of $R_{\rm L}$. Both resonators have the same resonance frequency $\omega_0 = 1/\sqrt{L_{\rm tx}C_{\rm tx}} = 1/\sqrt{L_{\rm rx}C_{\rm rx}}$, where $L_{\rm tx}$ and $L_{\rm rx}$ are inductances of Tx ad Rx, respectively. By employing the fundamental-harmonic linear approximation, we can write the system equation as

$$\begin{bmatrix} Z_{\rm tx} & {\rm j}\omega M_{\rm tx\text{-}rx} \\ {\rm j}\omega M_{\rm tx\text{-}rx} & R_{\rm L}+Z_{\rm rx} \end{bmatrix} \begin{bmatrix} I_{\rm tx} \\ I_{\rm rx} \end{bmatrix} = \begin{bmatrix} V_{\rm s} \\ 0 \end{bmatrix} \tag{1}$$

where $Z_i = R_i + {\rm j}X_i$, $X_i = \omega L_i - 1/C_i$ ($i = {\rm tx}, {\rm rx}$), $R_{\rm tx}$ and $R_{\rm rx}$ are the parasitic resistances of the coils, and $M_{\rm tx\text{-}rx}$ is the mutual inductance between the coils. One can easily find the currents in Tx and Rx ($I_{\rm tx}$ and $I_{\rm rx}$, respectively) at the resonant

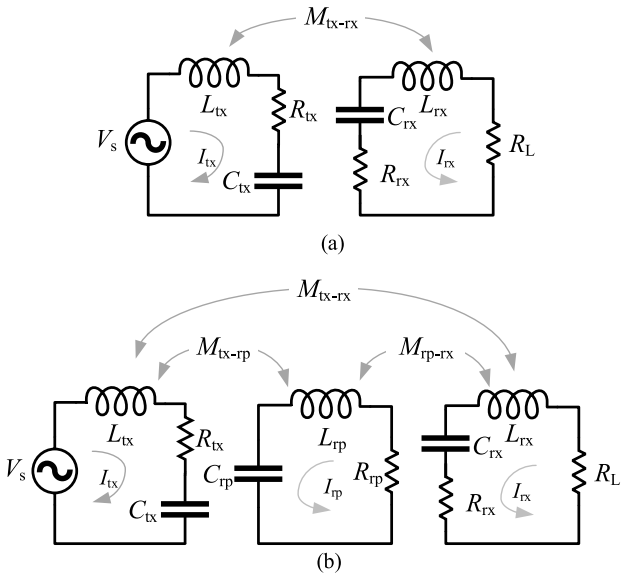

FIGURE 1. Equivalent circuit model of the wireless power transfer systems; (a) Two-coil system, and (b) WPT system with a repeater.

frequency ω_0 as

$$I_{tx} = \frac{V_s\,(R_{rx} + R_L)}{\omega_0^2 M_{tx\text{-}rx}^2 + R_{tx}\,(R_{rx} + R_L)},$$
$$I_{rx} = \frac{-j\omega_0 M_{tx\text{-}rx} V_s}{\omega_0^2 M_{tx\text{-}rx}^2 + R_{tx}\,(R_{rx} + R_L)}. \quad (2)$$

With the intention of understanding the multi-Tx WPT system, let us analyze the characteristics of I_{tx} and I_{rx} with respect to the change of $M_{tx\text{-}rx}$. For a given source voltage V_s, the maximum current in the Rx flows when $M_{tx\text{-}rx} = \sqrt{R_{tx}\,(R_{rx} + R_L)}/\omega_0$ (termed as crtical mutual coupling [5]), which essentially corresponds to a particular Rx position. When the Rx moves away from this critical coupling position, the Rx current decreases regardless of the Tx current. However, the Tx current increases with the decrease of $M_{tx\text{-}rx}$. Decreasing $M_{tx\text{-}rx}$ implies that Rx moves away from the Tx. When $M_{tx\text{-}rx}$ is small, Tx current is much higher than the Rx current, which leads to very low efficiency and a possibility of short circuit of the source. On the other hand, when Rx moves towards the Tx from the critical coupling position, both Tx and Rx current decreases.

In a multi-Tx WPT scenario, transmitters that are farther from the receiver should have smaller currents compared to those closer to the receiver. However, the characteristics of I_{tx} and I_{rx} of 2-coil WPT are completely opposite to what we want to achieve. Therefore, one should continuously detect the position of the Rx and control the Tx currents, which require additional sensing circuits and complex control approaches. Hence, the simple 2-coil WPT system is not promising for extending to multi-Tx WPT systems.

B. WPT SYSTEM WITH A REPEATER

Now, let us analyze a 3-coil WPT system with an additional intermediate repeater (Rp). The equivalent circuit of the 3-coil WPT system is shown in Fig. 1(b). The resonance frequency of the repeater is identical to the other two: $\omega_0 = 1/\sqrt{L_{tx}C_{tx}} = 1/\sqrt{L_{rp}C_{rp}} = 1/\sqrt{L_{rx}C_{rx}}$ where the subscript rp refers to the repeater.

We employ Kirchhoff's voltage law to define the system equation as

$$\begin{bmatrix} Z_{tx} & j\omega M_{tx\text{-}rp} & j\omega M_{tx\text{-}rx} \\ j\omega M_{tx\text{-}rp} & Z_{rp} & j\omega M_{rp\text{-}rx} \\ j\omega M_{tx\text{-}rx} & j\omega M_{rp\text{-}rx} & R_L + Z_{rx} \end{bmatrix} \begin{bmatrix} I_{tx} \\ I_{rp} \\ I_{rx} \end{bmatrix} = \begin{bmatrix} V_s \\ 0 \\ 0 \end{bmatrix}. \quad (3)$$

After solving (3), one can find the current in each coil. Assuming identical Tx and repeater coils (i.e $R_{tx} = R_{rp} = R$) and that the parasitic resistance of the Rx is much smaller compared to the load impedance ($R_L \gg R_{rx} \rightarrow R_L + R_{rx} \approx R_L$), the coil currents at the resonant frequency can be written as

$$I_{tx} = \frac{(M_{rp\text{-}rx}^2\omega_0^2 + RR_L)V_s}{A},$$
$$I_{rp} = \frac{-jV_s\omega_0 M_{tx\text{-}rp}R_L\left(1 - j\frac{\Delta}{2}\right)}{A},$$
$$I_{rx} = \frac{-jV_s(M_{tx\text{-}rx}R\omega_0) - jM_{rp\text{-}rx}M_{tx\text{-}rp}\omega_0^2}{A}, \quad (4)$$

where

$$A = R^2R_L + R\omega_0^2(M_{tx\text{-}rx}^2 + M_{rp\text{-}rx}^2) + M_{tx\text{-}rp}^2R_L\omega_0^2\,(1 - j\Delta),$$
$$\text{and } \Delta = \frac{2M_{tx\text{-}rx}M_{rp\text{-}rx}\omega_0}{M_{tx\text{-}rp}R_L}. \quad (5)$$

When the mutual inductance $M_{tx\text{-}rx} \ll M_{tx\text{-}rp}$, the term $\Delta \ll 1$. This mutual inductance relation can be easily realized when the distance between Tx and the repeater is smaller than the distance between Tx and Rx. Under the condition of $\Delta \ll 1$ and neglecting the parasitic resistance of the coils, i.e., $R \approx 0$, (4) can be simplified to

$$I_{tx} = \frac{M_{rp\text{-}rx}^2 V_s}{M_{tx\text{-}rp}^2 R_L},$$
$$I_{rp} = \frac{-jV_s}{\omega_0 M_{tx\text{-}rp}},$$
$$I_{rx} = \frac{-M_{rp\text{-}rx}V_s}{M_{tx\text{-}rp}R_L}. \quad (6)$$

We can observe an interesting characteristic in (6). The Rx current is proportional to $M_{rp\text{-}rx}$, while the Tx current is proportional to $M_{rp\text{-}rx}^2$, which is totally different from the characteristics of the 2-coil WPT system. When the mutual coupling between the repeater and the Rx increases, the currents in both Tx and Rx increase. This is in fact an essential and desired property for multi-Tx WPT. We see that when the receiver current is small (the receiver is far away or loaded with a high-resistance load), the current in the primary coil is suppressed while the repeater coil is still strongly excited. In the limiting case $R_L \rightarrow \infty$, the Tx current tends to zero. This practically useful feature has an interesting analogy with superlenses based on the use of resonant particles [20], [21]. Also in that device, the current in the first resonator (here we

excite it directly by a voltage source) is suppressed, while the current in the second resonator (our repeater) is enhanced, transferring the fields behind the arrays. Importantly, the repeater current is non-singular even in the limit of negligible losses and absent receiver. It should be noted that a similar behavior can be obtained using high-order compensator networks (e.g., LCC-series compensator in [24]), which requires additional lumped inductor(s). However, the realization of additional compensator inductors is challenging because of the undesirable coupling between them and Tx coil, and high additional losses. Particularly, for high-frequency WPT, the use of high-order compensators is not an effective approach as the use of ferrites is not practical for inductors.

It should also be highlighted that the output voltage $V_{\mathrm{L}} = I_{\mathrm{rx}} R_{\mathrm{L}}$ is independent of the load impedance R_{L} according to (6). When the Rx position is fixed, the 3-coil WPT system is equivalent to a voltage source applied across the load. We exploit these characteristics of 3-coil WPT to realise a self-tuning multi-Tx WPT system to freely positioned receivers.

TABLE 1. Parameters of Coils in WPT system.

Parameter	Value
Diameter	100 mm
Number of turns	8
Pitch between turns	4 mm
Diameter of wire	2 mm

Before moving to the multi-Tx WPT scheme, let us consider a numerical example of a 3-coil WPT system with three identical coils (the coil parameters are defined in Table 1) in order to validate the above analytical results and approximations. The distance between the Tx to the repeater should satisfy the condition $\Delta \ll 1$ while providing strong coupling between Tx and Rp. Therefore, the distances between the Tx to the repeater and the repeater to the Rx are set to 10 mm and 50 mm, respectively. In this example, $\Delta \approx 0.1$, which meets the requirement of (6). The normalized coil currents using the full analytical form in (4) are compared with the simplified derivation in (6). It is important to point out that both the full analytical and simplified-derivations results are normalized to the maximum repeater current, which can clearly show the relative relations of currents regardless of the power rating based on the linearity of the WPT system. The results shown in Fig. 2 verify the accuracy of the simplification. We can also observe that the Tx current decreases with Rx misalignment while keeping the repeater current almost constant. Therefore, we can exploit this property of the 3-coil WPT to achieve automatic power channeling in a multi-Tx WPT, which will be discussed in detail in the following section.

III. MULTI-TRANSMITTER AND MULTI-REPEATER SYSTEM

A. SYSTEM CONFIGURATION

Let us consider a multi-Tx WPT system consisting of multiple transmitter-repeater pairs. Each pair is referred to as a

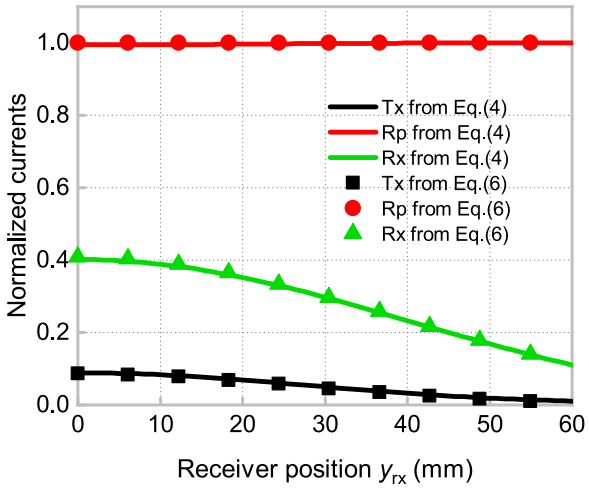

FIGURE 2. Normalized coil currents in the Tx, repeater (Rp), and the Rx of the 3-coil WPT systems versus the receiver position in *y*-direction.

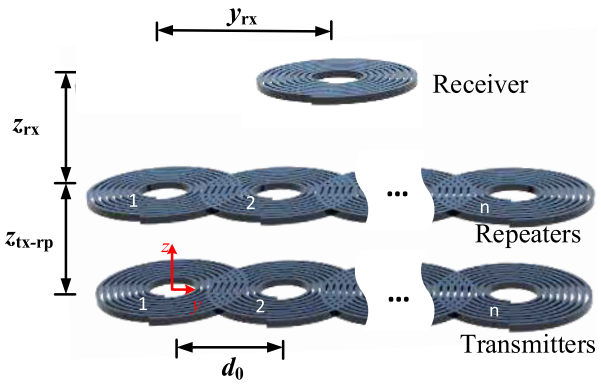

FIGURE 3. The coil arrangement of the multi-Tx WPT system.

channel. We also assume that coupling between all the coils except ones in the same channel are negligibly small. Now, the multi-Tx WPT system comprises a set of independent 3-coil WPT channels. This is again analogous to the main principle of superlenses based on resonant arrays. Also in those devices, the resonators in each array should be as weakly coupled to each other as possible, so that any distribution of currents over the array resonators corresponds to a resonant mode at the operational frequency. This property ensures creation of independent, point-to-point energy channels across the "lens". Note that, according to the above discussion, the current in a particular Tx decreases when the Rx is moved away from it.

The geometrical configuration can be in any form, for example, 1D linear array, 2D coil pad, or even a 3D arrangement. The only requirement is to have negligible cross coupling between the channels. For example, a coil arrangement of a 1D linear array is shown in Fig. 3 and the Rx can be positioned (or moved) along the array. Equivalent circuit of such multi-channel WPT system is illustrated in Fig. 4. We design the Tx and repeater arrays with partially overlapping coils to ensure zero mutual coupling between the adjacent coils. All the coils are chosen to be identical circular spirals with the design parameters given in Tables 1 and 2. The working

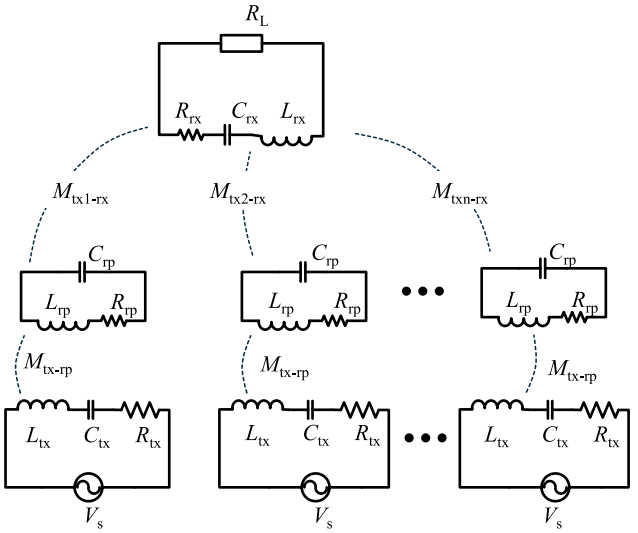

FIGURE 4. The equivalent circuit of the multi-Tx WPT system.

TABLE 2. Parameters of coil arrangement.

Parameters	Values
Distance between two adjacent coils (d_0)	57.55 mm
Distance between transmitter and repeater array ($z_{\text{tx-rp}}$)	10 mm
Distance between repeater array and receiver (z_{rx})	20 mm
	50 mm

frequency of the WPT system is chosen to be at 1 MHz and a series tuning capacitor is connected with each coil to tune the resonant frequencies to the working frequency. The transmitters connected in parallel and are excited by a voltage source.

B. ANALYSIS OF THE MULTI-TX WPT SYSTEM

For the analysis of the multi-Tx WPT system, we assume that the WPT system consists of n independent channels. Let us start with the analytical derivation of Rx current I_{rx} as a function of currents in the Txs and the repeaters. Using the equivalent circuit analysis, the Rx current I_{rx} is expressed as

$$I_{\text{rx}} = -\frac{\sum_{i=1}^{n} \text{j}\omega_0 M_{\text{tx}i\text{-rx}} I_{\text{tx}i} + \sum_{i=1}^{n} \text{j}\omega_0 M_{\text{rp}i\text{-rx}} I_{\text{rp}i}}{R_{\text{L}} + R} \tag{7}$$

where the subscript i refers to the i^{th} Tx or repeater coil. The output power at the load P_{out} is defined as

$$P_{\text{out}} = |I_{\text{rx}}|^2 R_{\text{L}}, \tag{8}$$

and the power transfer efficiency η of the WPT system is defined as

$$\eta = \frac{|I_{\text{rx}}|^2 R_{\text{L}}}{\sum_{i=1}^{n} |I_{\text{tx}i}|^2 R + \sum_{i=1}^{n} |I_{\text{rp}i}|^2 R + |I_{\text{rx}}|^2 (R + R_{\text{L}})}. \tag{9}$$

We assume that the channels are independent and the mutual coupling between Txs and the Rx is much weaker than that of the corresponding repeaters and the Rx. As we discussed in Section II, the power contribution directly from Txs to the Rx is very small compared to that from repeaters to the Rx. Therefore, we can approximate the currents in each coil individually by extending (6). This way, we can obtain the output power of the system as

$$\begin{aligned} P_{\text{out}} &= \frac{V_{\text{s}}^2}{k_{\text{tx-rp}}^2 R_{\text{L}}} \left(\sum_{i=1}^{n} k_{\text{rp}i\text{-rx}} \right)^2, \\ k_{\text{tx-rp}} &= \frac{M_{\text{tx-}rp}}{\sqrt{L_{\text{tx}} L_{\text{rp}}}}, \\ k_{\text{rp}i\text{-rx}} &= \frac{M_{\text{rp}i\text{-rx}}}{\sqrt{L_{\text{rp}i} L_{\text{rx}}}}, \end{aligned} \tag{10}$$

where $k_{\text{tx-rp}}$ and $k_{\text{rp}i\text{-rx}}$ are the coupling coefficients between Tx-repeater pairs in each independent channel and between the i^{th} repeater and the Rx, respectively.

In order to characterize the efficiency, we separate the loss contributions from the different segments of the system, i.e, the Tx array, the repeater array, and the Rx. To this end, we define loss ratios for each segment ($\xi_{\text{tx,rx,rp}} = P_{\text{tx,rx,rp}}/P_{\text{out}}$) as the ratios between the power losses in each segment and the output power (P_{out}). Substituting (6) into (9), the efficiency of the system can be simplified to

$$\begin{aligned} \eta &= \frac{1}{1 + \xi_{\text{tx}} + \xi_{\text{rx}} + \xi_{\text{rp}}}, \\ \xi_{\text{tx}} &= \frac{\left(\sum_{i=1}^{n} k_{\text{rp}i\text{-rx}}^4 \right)}{\Gamma k_{\text{tx-rp}}^2 \left(\sum_{i=1}^{n} k_{\text{rp}i\text{-rx}} \right)^2}, \\ \xi_{\text{rp}} &= \frac{n\Gamma}{Q^2 \left(\sum_{i=1}^{n} k_{\text{rp}i\text{-rx}} \right)^2}, \\ \xi_{\text{rx}} &= \frac{1}{\Gamma}, \quad \text{and} \quad \Gamma = \frac{R_{\text{L}}}{R}, \end{aligned} \tag{11}$$

where $Q = \omega_0 L/R$ is the unloaded quality factor of the coil, Γ is the ratio between the load resistance (R_{L}) and the coil resistance (R), which is generally much greater than unity, i.e., $\Gamma \gg 1$.

To maximize the efficiency in (11), one should minimize all the loss ratios. The loss ratio of the Tx array ξ_{tx} is much smaller compared to the other two loss ratios because of the fourth-order coupling summation term in the numerator and $\Gamma \gg 1$. The highest loss contribution comes from the repeaters, which can be decreased by increasing the sum of the coupling terms, or by increasing the coil quality factor. In order to evaluate the output power and the efficiency characteristics at different Rx positions, let us consider an Rx that moves along the Tx array, as illustrated in Fig. 3. When the Rx moves, the mutual coupling between each repeater to the Rx $k_{\text{rp}i\text{-rx}}$ changes, but the sum terms, $\sum_{i=1}^{n} k_{\text{rp}i\text{-rx}}$ and $\sum_{i=1}^{n} k_{\text{rp}i\text{-rx}}^4$ remain almost constant because a reduction of one coupling coefficient is compensated by an increase of another. Therefore, a nearly constant output power and high efficiency can be achieved. We can notice from (11) that

the repeater loss ratio ξ_{tx} increases with the increase of n. This means that the losses in the repeaters will increase with the increase of number of Txs, which will slightly decrease efficiency.

The optimal load resistance that gives maximum efficiency $R_{L\text{-opt}}$ can be evaluated as

$$R_{L\text{-opt}} = \frac{QR}{k_{tx\text{-}rp}} \sqrt{\frac{k_{tx\text{-}rp}^2 \left(\sum_{i=1}^{n} k_{rpi\text{-}rx}\right)^2 + \sum_{i=1}^{n} k_{rpi\text{-}rx}^4}{n}} \tag{12}$$

and the maximum efficiency η_{max} when the load impedance is optimal (i.e. $R_L = R_{L\text{-opt}}$) can be expressed as

$$\eta_{max} = \frac{1}{1+\frac{2}{Q}\sqrt{n\left(\frac{1}{\sum_{i=1}^{n} k_{rpi\text{-}rx}} + \frac{\sum_{i=1}^{n} k_{rpi\text{-}rx}^4}{k_{tx\text{-}rp}\left(\sum_{i=1}^{n} k_{rpi\text{-}rx}\right)^4}\right)}}. \tag{13}$$

The performance characteristics are further evaluated using a numerical example of 4-Tx array in the following section.

C. NUMERICAL VERIFICATION

We consider a 4-Tx WPT system as an example to validate the properties of automatic power channeling. The design parameters of the coils and the system are given in Table 1 and Table 2, respectively. The coupling coefficients between the coils are numerically calculated using the circular loop approximation as proposed in [25]. The coupling coefficient variations with respect to the lateral displacement between the WPT coils are illustrated in Fig. 5. The adjacent coils are spaced 57.55 mm away from each other, which is the uncoupling distance (d_0), corresponding to zero mutual inductance (see the line marked $z = 0$ in Fig. 5). It can also be observed from Fig. 5 that the coupling coefficients for non-adjacent Tx and repeater coils (indicated as $2d_0$ and $3d_0$) are negligibly small (less than 0.026) and the assumption of independent channels is valid.

The numerically calculated currents (normalized to the maximum repeater current) in Txs, Rps, and Rx with respect to the Rx position are shown in Fig. 5. In order to make the positions of channels clearer, we normalize the y-coordinates of the receiver position (y_{rx}) by the separation between two adjacent channels as y_{rx}/d_0. The receiver position varies from the center of Channel 1 (i.e., aligned to Tx1) to the center of Channel 4 (i.e., aligned to Tx4). The continuous lines correspond to the practical setup when all the cross-coupling terms are considered, and the dashed lines correspond to the ideal setup when all the cross-coupling terms are assumed to be zero. For the ideal structure, there is no coupling between any two coils belonging to two different channels, while for the practical set-up, two adjacent coils of transmitters or repeaters are positioned with uncoupling displacement d_0, but the mutual coupling still exists between non-adjacent coils. As shown in Fig. 5, the currents of the practical design (line) is closely following the results for the ideal condition (dashed line). The results verify that the cross-coupling terms are negligibly small and the solutions follow the ideal profile.

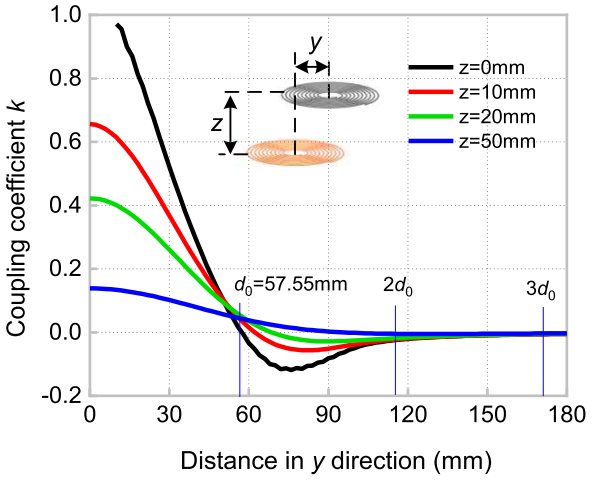

FIGURE 5. Coupling coefficient between two coils versus their displacement in y-direction.

Since the Tx coils are fed by an ideal voltage source, the input powers are proportional to the corresponding input currents. Therefore, let us now analyze the Tx current profiles at different Rx positions. For example, when the Rx moves away from Tx1, the current in Tx1 decreases while the current in Tx2 gradually increases. When the Rx is aligned to Tx2, the current in Tx2 reaches its peak, and the currents in all the other Txs are negligibly small. When the position of the Rx is in-between two Txs, the currents in the nearest Txs are identical meaning that the two Txs equally contribute to the power transfer. When the Rx moves along the Tx array, the currents in the four transmitter coils are adjusted automatically to transfer power optimally to the Rx. In the view of power channeling, four independent channels are automatically switched in conjunction with the position of the receiver. On the other hand, the Rp coils are strongly excited with high currents and the Rp currents remain almost constant for various Rx position (see Fig. 6(b)). Due to the edge effect and cross coupling in practical WPT systems, the currents in the two repeaters that locate at two sides of the planar array (channels 1 and 4) are slightly smaller than the currents in the two middle repeaters (channels 2 and 3). Most importantly, we can notice from Fig. 6(b) that the variation in the Rx current is very small. On the other hand, the output power is proportional to square of Rx current through the resistive load (see (8)). This result means that we achieve almost constant output power regardless of Rx position.

In order to further compare the characteristics of the proposed power channeling approach and conventional multi-coil systems, Tx currents in the corresponding conventional 4-transmitter coils system are plotted in Fig. 7, where the currents are normalized to the same value as that of Fig. 5(a). As we explained earlier, when the receiver is far away from a transmitter, the current in the Tx of conventional

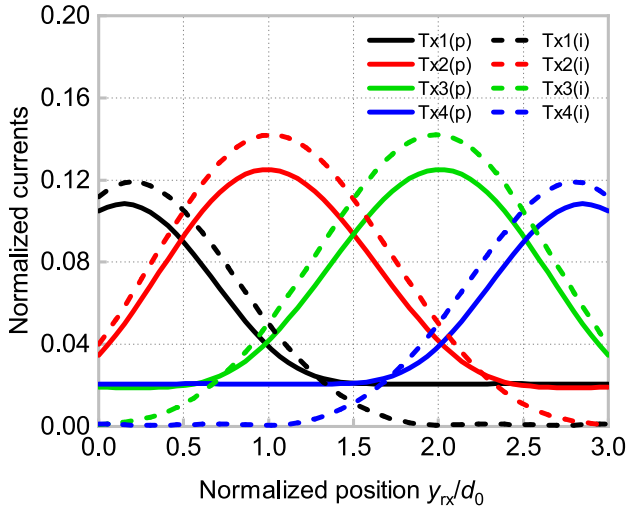

(a)

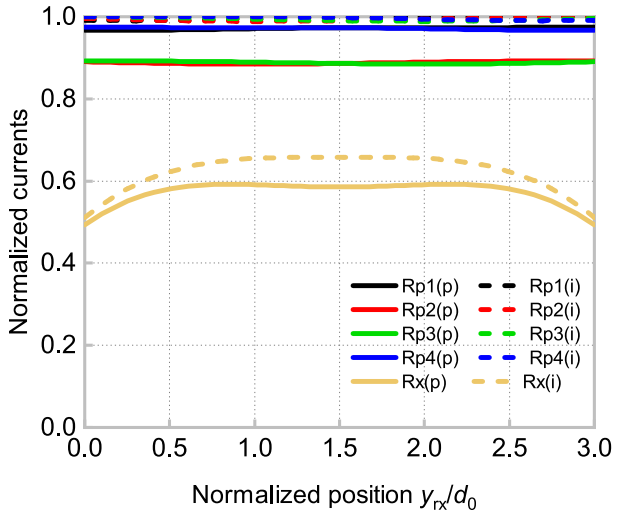

(b)

FIGURE 6. The variation of coil currents versus the normalized position to the receiver ($z_{rx} = 50$ mm). Lines indicated by 'p' correspond to the practical WPT system including all the cross coupling terms. Dashed lines indicated by 'i' correspond to the ideal scenario with the assumption of zero-coupling between the channels.; (a) Transmitter currents, and (b) Repeater and receiver currents.

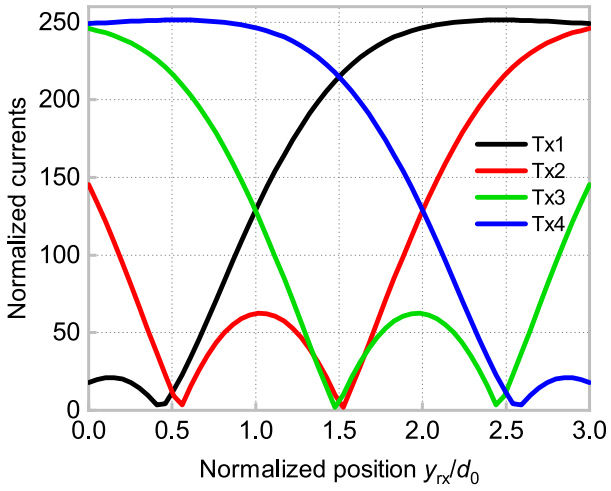

FIGURE 7. The variation of transmitter coil currents versus the normalized position to the receiver ($z_{rx} = 50$ mm) for the conventional multi-Tx WPT system.

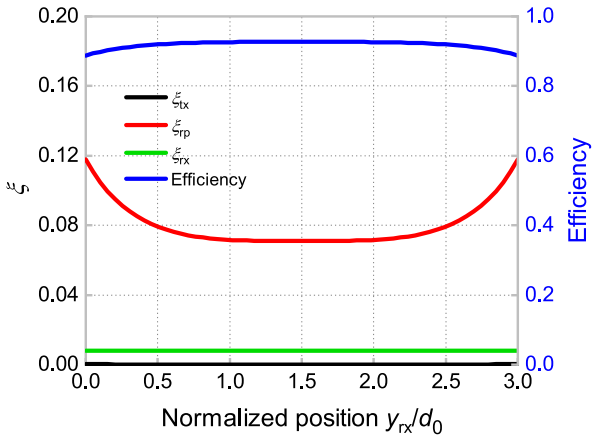

FIGURE 8. Power loss ratio and the efficiency variations against the receiver position in y-direction (coordinates are normalized to the channel separation d_0, and $z_{rx} = 50$ mm).

systems increases to a very high level, which is unacceptable in practical application.

Next, let us move to the analysis of the system efficiency with respect to the Rx position. The variation of loss ratios and the efficiency for different Rx positions are illustrated in Fig. 8. The overall efficiency is maintained above 90%. As we discussed in the previous section, the highest loss contribution is from the repeater array while the loss ratio of the Tx array is very small. Dissipation losses in Rp coils carrying strong currents can be mitigated using high-Q repeater coils. Therefore, the results verify that the proposed power channeling approach not only maintains constant power at the receiver, but also achieves high efficiency.

Finally, we discuss the effect of the number of channels to the power stability and efficiency. The normalized Rx current (normalized to the repeater current similarly to the above) and efficiency variations for different numbers of channels n are shown in Fig. 9. We can easily see that the output current (as well as the output power) is robust throughout the coverage of the array for different number of channels. We note that the increase of the number of channels allows covering a larger area, though by the price of a slight decrease in efficiency.

IV. EXPERIMENTAL VERIFICATION

Now, we move to the experimental verification of the proposed WPT system with the capability of automatic power channeling. The experimental setup is shown in Fig. 10, and includes four transmitters, four repeaters, and one receiver. All the coil parameters are chosen to match Table 1, and the coils are wounded using the Litz wire. The self-inductance and resistance of the coils were measured using an Agilent4284A LCR meter, and the measured results are shown in Table 3. The working frequency of the WPT system is chosen to be at 1 MHz (note that there is no fundamental limitation on the operational frequency), and series capacitors are added to each coil to make the coil resonant close to 1 MHz, and

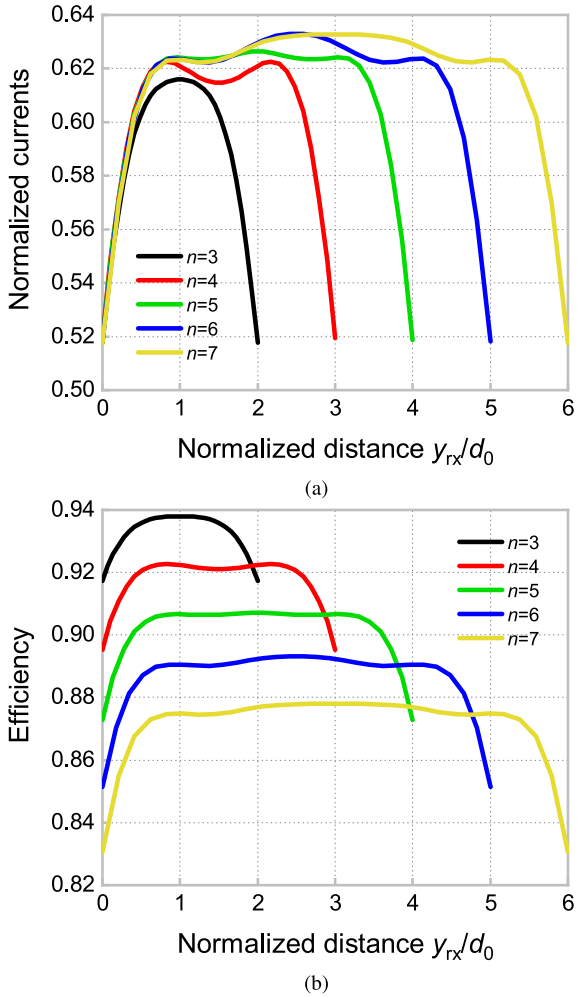

FIGURE 9. Receiver currents (normalized to the maximum repeater current used in Fig. 6(b)) and efficiency against the receiver position in y-direction (coordinates are normalized to the channel separation d_0, and $z_{rx} = 50$ mm), n is the number of Tx coils.; (a) Receiver currents, and (b) efficiency.

TABLE 3. Measured parameters of the WPT coils.

	Inductance (μH)	Resistance (mΩ)	f_0 (MHz)
Tx1	4.64	55	0.9972
Tx2	4.69	53	0.9968
Tx3	4.69	55	0.9990
Tx4	4.90	67	0.9990
Rp1	4.70	49	1.0024
Rp2	4.58	52	0.9930
Rp3	4.61	57	0.9988
Rp4	4.73	65	1.0024
Rx	4.47	42	1.0020

the experimentally measured resonant frequencies are given in Table 3. In order to make the mutual inductance of each pair of adjacent coil to be zero, the distance between two neighbour coil is fixed to 57.55 mm, based on the results in Fig. 5. The measured mutual inductance of two adjacent coils was less than 75 nH, which is negligible compared to the main coupling terms. Measured coupling coefficients between repeater and receiver, and transmitter and receiver are shown in Fig. 11. Coupling coefficient of Tx and Rp is

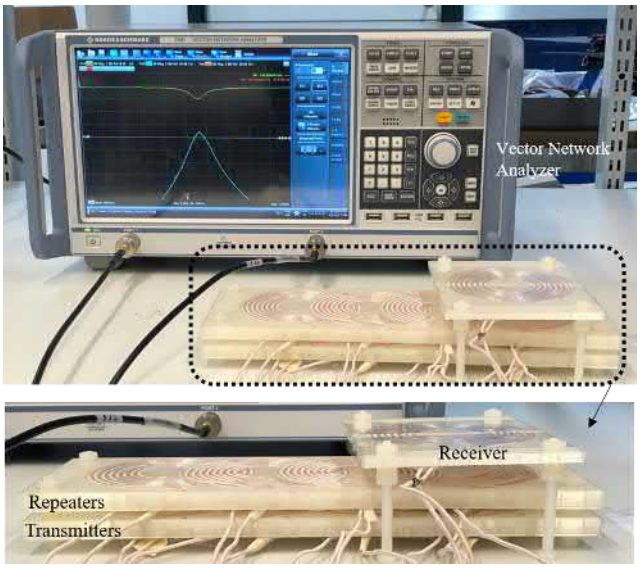

FIGURE 10. The experimental setup.

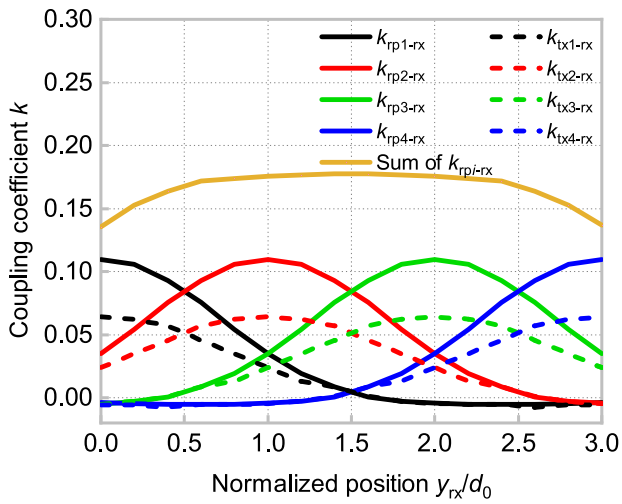

FIGURE 11. The measured mutual coupling coefficients against the normalized position to the receiver ($z_{rx} = 50$ mm).

around 0.7, and coupling values satisfy the condition $\Delta \ll 1$ for all the Rx positions considered. The receiver moves along the y-axis from the center of Tx1 (i.e., Channel 1) to the center of Tx4 (Channel 4). The parameters of the experimental setup correspond to the WPT system described in the previous section as presented in Table 2.

Next, the performances of the experimental prototype are evaluated with respect to receiver positions along the Tx array. The measurements are carried out using a vector network analyzer (VNA) where all the Txs are connected in parallel to Port 1 and the Rx is connected to Port 2. The two-port measurement using VNA is limited to the load impedance of 50 Ω. Therefore, the measured two-port network parameters are post-processed in Keysight Advanced Design System tool [26] by simulating the circuit for different load impedance values, as presented in [27]. Fig. 12 shows the variation of the measured efficiency with respect to the load impedance when

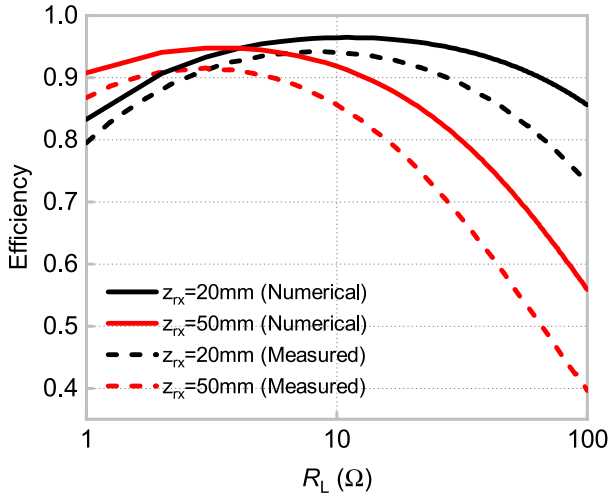

FIGURE 12. Efficiency against the load resistance when the z-distance between the repeater array and the receiver is 20 mm and 50 mm.

the receiver position is fixed at the center of the planar array (i.e., $y_{rx}/d_0 = 1.5$). We can see that the measured efficiency profile agrees well with the numerical results. The calculated values of the optimal load resistance from (12) are 7.88 Ω and 3.38 Ω for 20 mm and 50 mm distances between the repeater array and the receiver along the z-axis, which are in excellent agreement with the experimental and numerical results in Fig. 12. As an example, we choose 10 Ω as the load resistance to obtain relatively high efficiency for both $z_{rx} = 20$ mm and $z_{rx} = 50$ mm.

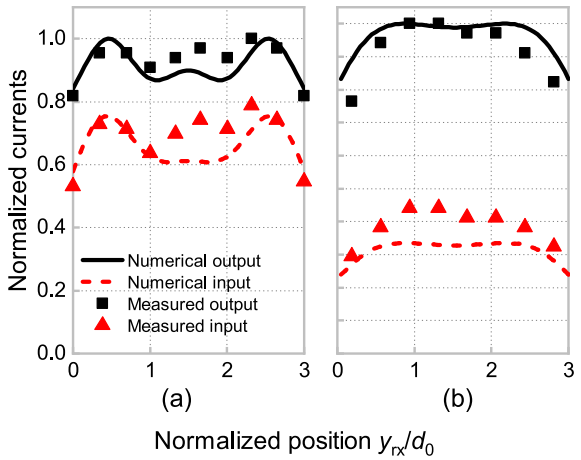

FIGURE 13. Normalized input current (i.e., the sum of all Tx currents) and the receiver current against the position of the receiver when the z-distance between the repeater array and the receiver is (a) 20 mm, and (b) 50 mm.

Fig. 13 shows the normalized input current (i.e., the sum of all the Tx currents) and the normalized receiver current with respect to the receiver position y_{rx}/d_0. The numerically calculated currents are normalized to the maximum receiver current, and the measured currents are normalized to the measured maximum receiver current. Due to the constraint of two ports during the experiment, the individual currents in each transmitter coil cannot be obtained directly. However, it is noted that the measured input current is in good agreement with the numerical results, which validates the theoretical analysis. The inconsistency of the numerical and measured results could be due to mismatch in self-resonance frequencies of the individual coils given in Table 1, and additional losses in the experimental setup, such as losses in capacitors and connectors. However, the experimental results agree with the theoretical analysis, which proves the efficacy of the proposed approach. For example, when the Rx is closer to a certain Tx, the current in this Tx increases, which can be considered as an activated channel for power transfer. When the position of the receiver changes, four transfer channels are switched on and off accordingly. Therefore, the receiver current is almost constant when the receiver moves along the Tx array, which verifies the theoretical basis of the power channeling.

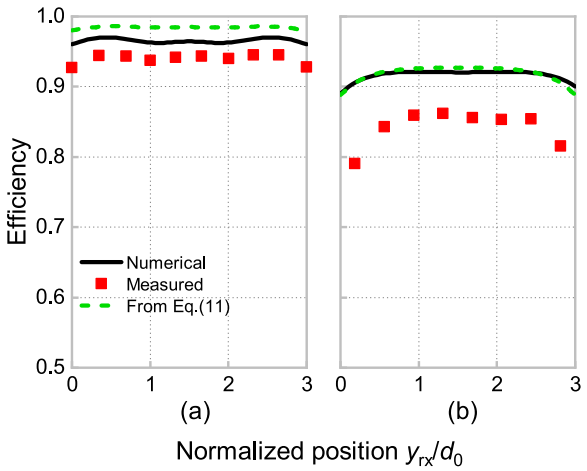

FIGURE 14. Efficiency variation against the normalized position of the receiver when the z-distance between repeater array and the receiver is (a) 20 mm, and (b) 50 mm.

The measured system efficiency variations versus the Rx position y_{rx}/d_0 are compared with the numerical calculations in Fig. 14 for $z_{rx} = 20$ mm and $z_{rx} = 50$ mm. We can see that the numerical calculations using full-form equations (i.e., using (9)) is in very good agreement with the simplified expression for the efficiency in (11), which verifies the simplification in (11). The maximum measured efficiency reaches 94.5% for $z_{rx} = 20$ mm and 86.2% for $z_{rx} = 50$ mm, and its variation is less than 2%. The experimental efficiencies are in good agreement with the numerical calculations. The disparity between the measured and numerical results is attributed to additional losses introduced in the experimental setup, such as losses in capacitors and connectors, and a slight mismatch in self-resonance frequencies of the individual coils, as shown in Table 3. Throughout the complete range of the receiver, the efficiency remains constant and at high level without having any sensing or active control circuits in the transmitter or receiver circuits.

In order to evaluate the benefits of the proposed method, the characteristics of the proposed approach are compared with a conventional multi-Tx WPT system without the

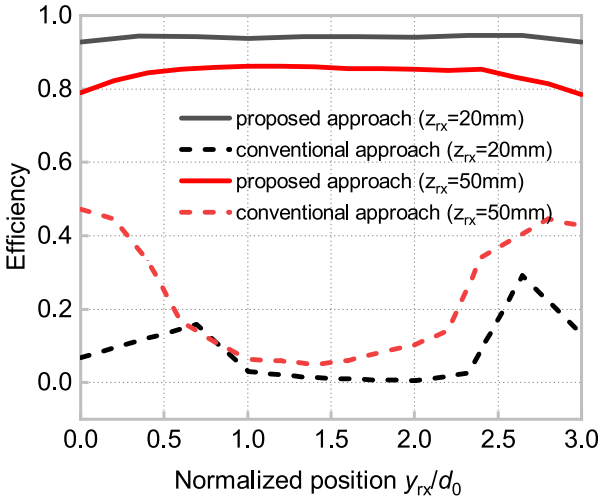

FIGURE 15. The comparison of the efficiency of the proposed WPT system with conventional multi-Tx WPT system when the *z*-distance between repeater array to the Rx (for the proposed WPT) or Tx array to the Rx (for the conventional WPT) is 20 mm and 50 mm.

repeater array. The efficiency variations against the Rx position for the proposed WPT system and the conventional WPT system are compared in Fig. 15. The conventional WPT system shows large efficiency variations as compared to the proposed WPT scheme. Most importantly, the efficiency of the conventional approach is very low because of the unoptimized distribution of Tx currents. As we discussed in Section II, this very low efficiency is due to undesirably high currents in Txs that are farther away from the Rx. Therefore, a continuous monitoring and control system is mandatory in conventional multi-Tx WPT systems to improve efficiency. Our method simplifies the system, since we eliminate the need of these monitoring and control circuits.

The experimental validation study is performed using a VNA as a power source, but the proposed approach remains valid for higher power rating as long as the source produces higher power. The design proposed in this paper can be applied to consumer electronics applications up to several hundreds of watts. Moreover, this new principle can be scaled to an arbitrary number of Tx coils in different arrangements (e.g., 2D pad-like arrangements) as long as uncoupled independent channels can be realized. However, we should note that with the increase of number of channels, the overall efficiency can be slightly reduced because of added losses in repeater coils. In addition, there may be unwanted electromagnetic exposure due to highly excited repeaters that are farther away from the receiver. In such cases, the following control strategy can be implemented to deactivate unused power channels: It is possible to fully deactivate ineffective Tx coils by measuring their current amplitude and switching them off if the current falls down below a certain threshold. This will deactivate the respective repeater, mitigating losses in the respective coil. Importantly, such simple control system does not need any sensors at the receiver side.

V. CONCLUSION

We have presented a self-tuning multiple transmitters WPT system, which always provides effective channels for optimal power delivery to freely positioned receivers. This property is achieved due to formation of independent power channels, linking the transmitters and the receiver. These channels gradually switch themselves on and off depending on the receiver position without any control or tuning. The requirements of realizing this feature are 1. All the cross couplings between channels are negligibly small, and 2. For a given channel, coupling between the repeater-Rx pair is much higher than that of the Tx-Rx pair. As long as the above two conditions are satisfied, the proposed self-tuning feature can be realized. We would like to highlight that particular coil arrangement and geometries presented in the paper are used as a proof-of-concept prototype. The efficiency, the input and receiver currents are measured for a system with four Tx coils and four repeater coils. The measured results agree well with the theoretical and the numerical values. The efficiency of the system reaches 94.5% and 86.2% for two different distances between the repeater array and the receiver, 20 mm and 50 mm, respectively. Stable and high efficiency is observed for changing receiver location, with the degree of variation less than 2%. Thanks to its simple structure and low cost, the proposed WPT system is a possible solution in many wireless charging applications, especially in consumer electronics. One limitation in the proposed coil arrangement is that the distance between the repeater array and the receiver must always be larger than the distance between the transmitters and repeaters to satisfy the second condition given above. In our current studies, we are working on new coil designs to overcome the limitation that the distance between Tx and Rx is large enough. We hope that the introduced and experimentally tested new principle of power channeling to enable free positioning of receivers in multi-Tx WPT systems without having any sensing or control circuits will be a contribution to power, industrial, and consumer electronics.

REFERENCES

[1] X. Liu and S. Y. Hui, "Optimal design of a hybrid winding structure for planar contactless battery charging platform," *IEEE Trans. Power Electron.*, vol. 23, no. 1, pp. 455–463, Jan. 2008.

[2] S. A. Mirbozorgi, H. Bahrami, M. Sawan, and B. Gosselin, "A smart multicoil inductively coupled array for wireless power transmission," *IEEE Trans. Ind. Electron.*, vol. 61, no. 11, pp. 6061–6070, Nov. 2014.

[3] U.-M. Jow and M. Ghovanloo, "Geometrical design of a scalable overlapping planar spiral coil array to generate a homogeneous magnetic field," *IEEE Trans. Magn.*, vol. 49, no. 6, pp. 2933–2945, Jun. 2013.

[4] W. X. Zhong, X. Liu, and S. Y. R. Hui, "A novel single-layer winding array and receiver coil structure for contactless battery charging systems with free-positioning and localized charging features," *IEEE Trans. Ind. Electron.*, vol. 58, no. 9, pp. 4136–4144, Sep. 2011.

[5] C. C. Mi, G. Buja, S. Y. Choi, and C. T. Rim, "Modern advances in wireless power transfer systems for roadway powered electric vehicles," *IEEE Trans. Ind. Electron.*, vol. 63, no. 10, pp. 6533–6545, Oct. 2016.

[6] S. A. Mirbozorgi, H. Bahrami, M. Sawan, and B. Gosselin, "A smart cage with uniform wireless power distribution in 3D for enabling long-term experiments with freely moving animals," *IEEE Trans. Biomed. Circuits Syst.*, vol. 10, no. 2, pp. 424–434, Apr. 2016.

[7] F. Jolani, Y.-Q. Yu, and Z. Chen, "A planar magnetically-coupled resonant wireless power transfer using array of resonators for efficiency enhancement," in *IEEE MTT-S Int. Microw. Symp. Dig.*, May 2015, pp. 1–4.
[8] J. W. Kim, H.-C. Son, D.-H. Kim, J.-R. Yang, K.-H. Kim, K.-M. Lee, and Y.-J. Park, "Wireless power transfer for free positioning using compact planar multiple self-resonators," in *Proc. IEEE MTT-S Int. Microw. Workshop Ser. Innov. Wireless Power Transmiss., Technol., Syst., Appl.*, May 2012, pp. 127–130.
[9] P. K. S. Jayathurathnage, A. Alphones, D. M. Vilathgamuwa, and A. Ong, "Optimum transmitter current distribution for dynamic wireless power transfer with segmented array," *IEEE Trans. Microw. Theory Techn.*, vol. 66, no. 1, pp. 346–356, Jan. 2018.
[10] S. Huh and D. Ahn, "Two-transmitter wireless power transfer with optimal activation and current selection of transmitters," *IEEE Trans. Power Electron.*, vol. 33, no. 6, pp. 4957–4967, Jun. 2018.
[11] S. Y. Hui, "Planar wireless charging technology for portable electronic products and qi," *Proc. IEEE*, vol. 101, no. 6, pp. 1290–1301, Jun. 2013.
[12] Y. Li, J. Hu, T. Lin, X. Li, F. Chen, Z. He, and R. Mai, "A new coil structure and its optimization design with constant output voltage and constant output current for electric vehicle dynamic wireless charging," *IEEE Trans. Ind. Informat.*, vol. 15, no. 9, pp. 5244–5256, Sep. 2019.
[13] A. Pacini, A. Costanzo, S. Aldhaher, and P. D. Mitcheson, "Load- and position-independent moving MHz WPT system based on GaN-distributed current sources," *IEEE Trans. Microw. Theory Techn.*, vol. 65, no. 12, pp. 5367–5376, Dec. 2017.
[14] W. Kim and D. Ahn, "Efficient deactivation of unused LCC inverter for multiple transmitter wireless power transfer," *IET Power Electron.*, vol. 12, no. 1, pp. 72–82, Jan. 2019.
[15] X. Dai, X. Li, Y. Li, and A. P. Hu, "Maximum efficiency tracking for wireless power transfer systems with dynamic coupling coefficient estimation," *IEEE Trans. Power Electron.*, vol. 33, no. 6, pp. 5005–5015, Jun. 2018.
[16] D. Kobayashi, T. Imura, and Y. Hori, "Real-time coupling coefficient estimation and maximum efficiency control on dynamic wireless power transfer for electric vehicles," in *Proc. IEEE PELS Workshop Emerg. Technol., Wireless Power (WoW)*, Jun. 2015, pp. 1–6.
[17] V. Jiwariyavej, T. Imura, and Y. Hori, "Coupling coefficients estimation of wireless power transfer system via magnetic resonance coupling using information from either side of the system," *IEEE J. Emerg. Sel. Topics Power Electron.*, vol. 3, no. 1, pp. 191–200, Mar. 2015.
[18] J. P.-W. Chow, H. S.-H. Chung, and C.-S. Cheng, "Use of transmitter-side electrical information to estimate mutual inductance and regulate receiver-side power in wireless inductive link," *IEEE Trans. Power Electron.*, vol. 31, no. 9, pp. 6079–6091, Sep. 2016.
[19] M. Mohammad and S. Choi, "Sensorless estimation of coupling coefficient based on current and voltage harmonics analysis for wireless charging system," in *Proc. IEEE Energy Convers. Congr. Expo. (ECCE)*, Oct. 2017, pp. 2767–2772.
[20] S. Maslovski, S. Tretyakov, and P. Alitalo, "Near-field enhancement and imaging in double planar polariton-resonant structures," *J. Appl. Phys.*, vol. 96, no. 3, pp. 1293–1300, Aug. 2004.
[21] P. Alitalo, C. Simovski, A. Viitanen, and S. Tretyakov, "Near-field enhancement and subwavelength imaging in the optical region using a pair of two-dimensional arrays of metal nanospheres," *Phys. Rev. B, Condens. Matter*, vol. 74, no. 23, 2006, Art. no. 235425.
[22] M. J. Freire and R. Marqués, "Planar magnetoinductive lens for three-dimensional subwavelength imaging," *Appl. Phys. Lett.*, vol. 86, no. 18, May 2005, Art. no. 182505.
[23] M. S. M. Mollaei and C. Simovski, "Dual-metasurface superlens: A comprehensive study," *Phys. Rev. B, Condens. Matter*, vol. 100, no. 20, Nov. 2019, Art. no. 205426.
[24] S. Zhou and C. C. Mi, "Multi-paralleled LCC reactive power compensation networks and their tuning method for electric vehicle dynamic wireless charging," *IEEE Trans. Ind. Electron.*, vol. 63, no. 10, pp. 6546–6556, Oct. 2016.
[25] Y. P. Su, X. Liu, and S. Y. R. Hui, "Mutual inductance calculation of movable planar coils on parallel surfaces," *IEEE Trans. Power Electron.*, vol. 24, no. 4, pp. 1115–1123, Apr. 2009.
[26] Keysight. *Advanced Design System (ADS)*. Accessed: 2019. [Online]. Available: https://www.keysight.com/en/pc-1297113/advanced-design-system-ads
[27] J. Kim, D.-H. Kim, and Y.-J. Park, "Analysis of capacitive impedance matching networks for simultaneous wireless power transfer to multiple devices," *IEEE Trans. Ind. Electron.*, vol. 62, no. 5, pp. 2807–2813, May 2015.

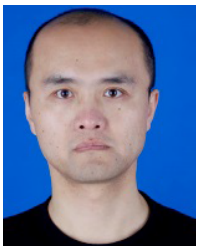

XIAOJIE DANG was born in Inner Mongolia, China. He received the B.S., M.S., and Ph.D. degrees in the electromagnetic field and microwave technology from Xidian University, Xi'an, China, in 2003, 2006, and 2011, respectively.

Since 2012, he has been with the School of Electronics Engineering, Xidian University, where he is currently a Lecturer. His research interests include metamaterials, metasurfaces, antennas, and wireless power transfer.

PRASAD JAYATHURATHNAGE (Member, IEEE) received the B.Sc. degree in electronics and telecommunications engineering from the University of Moratuwa, Moratuwa, Sri Lanka, in 2009, and the Ph.D. degree in electrical and electronics engineering from Nanyang Technological University, Singapore, in 2017.

He is currently a Postdoctoral Researcher with Aalto University, Espoo, Finland. His research interests include high-frequency power converters, wireless power transfer, and biomedical implants.

SERGEI A. TRETYAKOV (Fellow, IEEE) received the Dipl. Engineer-Physicist, Candidate of Sciences (Ph.D.), and D.Sc. degrees in radiophysics from Saint Petersburg State Technical University, Saint Petersburg, Russia, in 1980, 1987, and 1995, respectively. From 1980 to 2000, he was with the Department of Radiophysics, Saint Petersburg State Technical University. He is currently a Professor of radio science with the Department of Electronics and Nanoengineering, Aalto University, Espoo, Finland. He has authored or coauthored five research monographs and over 270 journal articles. His current research interests include electromagnetic field theory, complex media electromagnetics, metamaterials, and microwave engineering. He served as the Chairman of the Saint Petersburg IEEE Electron Devices/Microwave Theory and the Techniques/Antennas and Propagation Chapter, from 1995 to 1998, and the General Chair of the International Congress Series on Advanced Electromagnetic Materials in Microwaves and Optics (Metamaterials) and the President of the Virtual Institute for Artificial Electromagnetic Materials and Metamaterials (Metamorphose VI), from 2007 to 2013.

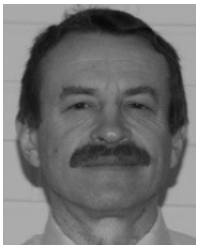

CONSTANTIN (KONSTANTIN) R. SIMOVSKI received the Ph.D. and Doctor of Sciences (HDR) degrees in physics and mathematics from the St. Petersburg State Polytechnic University, Saint Petersburg, Russia, in 1986 and 2000, respectively. He was with both industry and academic institutions in several countries. From 2001 to 2008, he was a Full Professor with the ITMO University, Saint Petersburg. Since 2008, he has been with Aalto University, Espoo, Finland, where he has been a Full Professor, since 2012. His current research interests include metamaterials for optical sensing and energy harvesting, thermal radiation and radioactive heat transfer on a nanoscale, antennas for magnetic resonance imaging, and wireless power transfer.